Article

An Adaptive Output Feedback Controller for Boost Converter

Xiaoyu Zhang, Wei He * and Yanqin Zhang

School of Automation, Nanjing University of Information Science and Technology, Nanjing 210044, China; 201913930055@nuist.edu.cn (X.Z.); 20211249162@nuist.edu.cn (Y.Z.)

* Correspondence: hwei@nuist.edu.cn; Tel.: +86-15895952178

Abstract: The main contribution of this paper is to propose an adaptive reduced-order state observer for boost converter to reconstruct the inductor current and load conductance. Note that the unknown parameter appears in the output dynamics, which poses a detectability obstacle, imposing a more stringent requirement on the system behavior. As a result, the design of an adaptive reduced-order state observer is more challenging. In this paper, using the dynamic extension technique, we transform the state observation into the parameter estimation. Constructing the parameter observer, the current and load conductance can be estimated. Introducing the estimated terms to a saturated PI passivity-based control, an adaptive output feedback saturated controller is presented. To assess the control performance, the simulation and experimental results are given.

Keywords: boost converter; reduced-order state observer; passivity-based control; stability analysis

1. Introduction

The DC–DC power converter is a type of energy transmission equipment for converting the DC voltage between sources and loads [1–3]. A boost converter is used to step up the voltage, which is widely used in electronic communication, aerospace, military equipment and other fields [4–6]. It is noted that its average model is a bilinear system, which makes the controller design more difficult. This fact is stated in [7,8]. The non-minimum phase property also poses a difficulty in the control scheme. Moreover, the load conductance changes along with the variation of the working operation. Therefore, being aware of the above problems, many researchers focus on this topic for addressing the control problem of the boost converter. Note that many results focus on the full-information control scheme. This means that two states of the system should be measurable. However, in some practical applications, although the inductor current is measurable, an output feedback controller is still desired for stabilizing the system using the only measurement of the output voltage. In this case, we only install one sensor to obtain the information of the output signal. Hence, the cost of power system can be clearly reduced and the reliability is improved.

Note that the zero dynamic system with respect to the current for the system is asymptotically stable. In the case, a first way to develop an output feedback control scheme is to adopt the indirect current control scheme [9–11]. It means that a controller is designed to ensure the current dynamic is asymptotically stable. Borrowing the property of the zero dynamic, the overall system is asymptotically stable. However, it should be pointed out that the implementation of such current-mode controllers may require prior knowledge of the load resistance and also demand more states, such as one or more currents in the feedback, which results in poor robustness performance.

The second way to address this problem is to present a controller for stabilizing this system which only relies on the output voltage. Note that this is different from the current-mode control and directly regulates the output voltage without considering the zero dynamic stability. In [12–15], a simplified output feedback controller without needing knowledge of the current is developed. The problem is that the stability analysis is based on the local linearization technique. In [16], the authors adopt the interconnection and

damping passivity based control technique to give an output feedback controller. Note that this controller is simple, so it can be easily implemented. Based on the periodic event-triggered method, a sliding mode dynamic output feedback controller design is applied to stabilize the boost converter [17,18].

The third way to propose a desired output feedback controller is to devise an observer to reconstruct the state. For example, in [19], a discrete time Luenburger observer is designed to estimate the current and then form a composite model predictive control. In [20], combining the current observer and an adaptive law, an output feedback control scheme is achieved. It is reported in [21] that the authors proposed an immersion and invariance (I&I) observer to estimate the system states. The problem is that the knowledge of load resistance is needed to construct the observer. An adaptive law seems to be designed to estimate it. Unfortunately, this does not work for boost converters since a detectability obstacle exists. Therefore, using the I&I technique, the result in [22] overcomes the detectability obstacle to an adaptive output feedback controller. In [23], the authors propose a full-order observer to estimate the state. However, in many practical applications, the reduced-order observer is desired for reducing the calculation. Moreover, the saturation problem of the control input is not addressed.

Motivating by the above problems, we adopt a PI passivity-based controller (PI-PBC) proposed in [24] to stabilize the boost converter. It is noted that this control method will provide a nice performance for the non-minimum phase and bilinear power converter system. Indeed, we do not need to locally linearize the nonlinear system and regulate the current for indirectly controlling output. It not only brings a simpler control structure, but also gives a nice control performance under the variable working condition. Due to the existence of the integral action, it can also obtain a nice robustness in practical application. A reduced-order state observer is designed for estimating the current and load conductance. The specific contributions of this paper are as follows:

- Inspired by the result [25], a saturated PI passivity-based controller (PI-PBC) is applied to stabilize the boost converter with the support of experiment validation. Note that an appropriate monotone transformation is introduced to address the saturation problem of the control input.
- Following the work [26], a reduced-order parameter estimation-based observer (PEBO) is devised to estimate the inductor current and load conductance.
- The simulation and experiment results are given to assess the performance of the proposed adaptive output feedback controller.

The remainder of the paper is organized as follows. The model and problem formation are presented in Section 2. Section 3 proposes the output feedback controller. The simulation and experimental results are provided in Section 4. The conclusion and future work are given in Section 6.

2. System Model and Problem Formation

2.1. The Model

Figure 1 corresponds to the topology of a boost converter. It is supposed that it works in continuous conduction mode. Adopting the state-space averaging method proposed in [27–29], its averaged model is given by

$$\begin{cases} L\dot{i} = -ri - (1-d)v + E, \\ C\dot{v} = (1-d)i - Gv, \end{cases} \tag{1}$$

where $i \in \mathbb{R}$ is an inductor current, $v \in \mathbb{R}$ is the output voltage, G is the conductance, E is the input voltage, L is the inductor, C is the capacitance, r is the parasitic resistance, and $d \in [0,1]$ is the duty ratio. The equilibrium set is described as

$$\mathcal{E}_{\texttt{boost}} = \{(i,v) \in \mathbb{R}^2 \mid ri^2 + Gv^2 - Ei = 0\}. \tag{2}$$
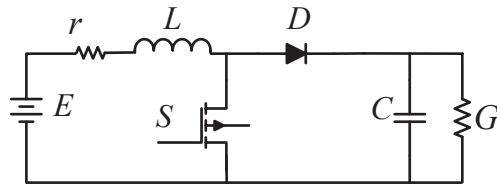
Figure 1. The circuit topology of DC–DC boost converter.

2.2. Problem Formation

In this paper, the main problem is to propose an output feedback control scheme for the boost converter. It means that the knowledge of the current and load conductance is not needed, and the output voltage is only measurable. The closed-loop system has the following features.

F1. The real information of the current and load conductance can be reconstructed via the designed observer. That is,

$$\lim_{t\to\infty} \hat{i}(t) = i(t), \lim_{t\to\infty} \hat{G}(t) = G(t). \tag{3}$$

F2. The control input is ensured to satisfy the set $d \in [0,1]$, in which the saturation problem is addressed. Under the saturation constraint, the closed-loop system is asymptotically stable. That is,

$$\lim_{t\to\infty} v(t) = v_\star, \tag{4}$$

with all signals bounded and initial conditions.

3. Adaptive Output Feedback Controller Design

Here, we follow the design steps to develop an output feedback controller. First, the load conductance G and the current i are assumed to be known. A saturated controller is developed to regulate the output voltage of the boost converter around the equilibrium. Second, based on the parameter estimation technique, a reduced-order adaptive state observer is designed to reconstruct the current and load conductance. Finally, an adaptive output feedback controller is formed by combining the state feedback controller and the designed observer.

Toward the controller design, the model (1) is expressed by the port-controlled Hamiltonian form

$$\dot{x} = (\mathcal{J}u - \mathcal{R})Qx + \zeta, \tag{5}$$

where $u = 1 - d$,

$$x = \begin{bmatrix} Li \\ Cv \end{bmatrix}, \mathcal{J} = \begin{bmatrix} 0 & -1 \\ 1 & 0 \end{bmatrix}, Q = \begin{bmatrix} \frac{1}{L} & 0 \\ 0 & \frac{1}{C} \end{bmatrix}, \mathcal{R} = \begin{bmatrix} r & 0 \\ 0 & G \end{bmatrix}, \zeta = \begin{bmatrix} E \\ 0 \end{bmatrix}.$$

The equilibrium set can be written as

$$\dot{x}_\star = (\mathcal{J}u_\star - \mathcal{R})Qx_\star + \zeta, \tag{6}$$

where $x_\star \in \mathcal{E}$.

3.1. Saturated Controller Design

First, before the controller design, we want to introduce a map to deal with the saturation problem of the control input. We define a map $q : \mathbb{R} \to \mathbb{R}$, which is strongly monotone and verify

$$(q(s+h) - q(s))^\top h > \eta \|h\|^2, \tag{7}$$

If (7) holds for $\eta = 0$, the map q is said to be monotone. We assume that

$$q(s+a) = q(s) + \psi(s, a), \tag{8}$$

where if $a = 0$, then $\psi(s, a) = 0$. Note that if q is sufficiently smooth, the following claim is satisfied.

$$(q(s+h) - q(s))^\top k = h^\top \frac{\partial q}{\partial s} k. \tag{9}$$

In this case, Equation (7) is equal to

$$h^\top \frac{\partial q}{\partial s} h \geq \eta \|h\|^2.$$

Using the above defined map, a saturated PI-PBC is proposed in the following proposition. Here, we assume i and G are known. The control input physically corresponds to a collection of modulation signals that are constrained to a closed set $\mathcal{U} \subset \mathbb{R}$.

Proposition 1. *A saturated controller is given by*

$$\begin{cases} \dot{z} = \tilde{y}, \\ u = q(-k_p \tilde{y} - k_i z), \end{cases} \tag{10}$$

where $q : \mathbb{R} \to \mathcal{U}$ is bounded, and the passive output is given by

$$\tilde{y} = \tilde{x}^T Q g_\star, \tag{11}$$

where $g_\star = \mathcal{J} Q x_\star$. It is ensured that the closed-loop system under the controller (10) is globally asymptotically stable with the equilibrium $(x, z) = (x_\star, -\frac{1}{k_i} u_\star)$ if, and only if,

$$\begin{cases} \varepsilon < \dfrac{2}{|g_\star| \sqrt{k_i Q}}, \\ \mathcal{R}_a > \max\{0, \dfrac{1}{4} b_a (\varepsilon g_\star g_\star^\top N_1)^{-1} b_a^\top \}, \end{cases} \tag{12}$$

where $\mathcal{R}_a := \mathcal{R} + k_p g_\star N_1 g_\star^\top + k_i \varepsilon g_\star g_\star^\top$, $b_a = -k_i \varepsilon \mathcal{R} g_\star - k_i N_1 g_\star - k_i N_2 g_\star - k_p k_i \varepsilon N_1 g_\star^\top Q g_\star g_\star^\top$. It is ensured that $N_1 = \frac{\partial q}{\partial s}(-k_i z_\star)$, $N_2 = \frac{\partial q}{\partial s}(k_i z_\star)$.

Proof. We define $w = -k_p \tilde{y} - k_i z$ and have $\tilde{w} = w - w_\star = -k_p \tilde{y} - k_i \tilde{z}$. In this case, the controller can be rewritten as $u = q(w)$. Based on the dynamics (5) and (6), the error dynamic can be given by

$$\begin{cases} \dot{\tilde{x}} = (\mathcal{J} u - \mathcal{R}) Q \tilde{x} + \tilde{u} g_\star \\ \tilde{y} = \tilde{x}^T Q g_\star, \end{cases} \tag{13}$$

where $\tilde{x} = x - x_\star, g_\star = \mathcal{J} Q x_\star, \tilde{u} = q(w) - q(w_\star)$. Note that $\dot{z} = \dot{\tilde{z}}, \dot{x} = \dot{\tilde{x}}$ since the equilibrium is constant. Next, we define the Lyapnuov function

$$W = \frac{1}{2} \tilde{x}^\top Q \tilde{x} + k_i \varepsilon \tilde{z} g_\star^\top Q \tilde{x} + \int_0^{\tilde{z}} (q(k_d \tau + k_i z_\star) - q(k_i z_\star)) d\tau. \tag{14}$$

Verifying the condition (12) and recalling that the map q is strongly monotone and $k_i > 0$, one has $W > 0$. Differentiating this function along the trajectory (13) yields

$$
\begin{aligned}
\dot{W} =& \tilde{x}^\top Q((Ju - \mathcal{R})Q\tilde{x} + \tilde{u}g_\star) + k_i \varepsilon \tilde{z} g_\star^\top Q((Ju - \mathcal{R})Q\tilde{x} + \tilde{u}g_\star) + k_i \varepsilon \tilde{x}^\top Q g_\star g_\star^\top Q\tilde{x} + (q(k_i z) \\
& - q(k_i z_\star))^\top \dot{z}, \\
=& - \tilde{x}^\top Q(\mathcal{R} + k_i \varepsilon g_\star g_\star^\top)Q\tilde{x} + k_i \varepsilon \tilde{z} g_\star^\top (Ju - \mathcal{R})Q\tilde{x} + k_i \varepsilon \tilde{z} g_\star^\top (q(\tilde{w} + w_\star) - q(w_\star))g_\star \\
& + \tilde{x}^\top Q(q(\tilde{w} + w_\star) - q(w_\star))g_\star + (q(k_i z_\star + k_i \tilde{z}) - q(k_i z_\star))\tilde{y}.
\end{aligned}
$$

Next, using (7) and (9) yields

$$
\begin{aligned}
\dot{W} =& - \tilde{x}^\top Q(\mathcal{R} + k_i \varepsilon g_\star g_\star^\top)Q\tilde{x} + \tilde{x}^\top Q\frac{\partial q}{\partial s}(w_\star)\tilde{w}g_\star + k_i \varepsilon \tilde{z} g_\star^\top \frac{\partial q}{\partial s}(w_\star)\tilde{w}g_\star - \tilde{z}k_i \frac{\partial q}{\partial s}(k_i z_\star)\tilde{y} \\
& - k_i \varepsilon \tilde{z} g_\star^\top \mathcal{R} Q\tilde{x}, \\
=& - \tilde{x}^\top Q(\mathcal{R} + k_p g_\star N_1 g_\star^\top + k_i \varepsilon g_\star g_\star^\top)Q\tilde{x} + \tilde{x}^\top Q(-k_i \varepsilon \mathcal{R} g_\star - k_i N_1 g_\star - k_i N_2 g_\star \\
& - k_p k_i \varepsilon N_1 g_\star^\top Q g_\star g_\star^\top)\tilde{z} - k_i \tilde{z} \varepsilon N_1 g_\star^\top Q g_\star k_i \tilde{z} \\
=& - \begin{bmatrix} Q\tilde{x}^\top \\ k_i \tilde{z} \end{bmatrix}^\top \begin{bmatrix} \mathcal{R}_a & \frac{1}{2}b_a \\ \frac{1}{2}b_a^\top & \varepsilon g_\star g_\star^\top N_1 \end{bmatrix} \begin{bmatrix} Q\tilde{x}^\top \\ k_i \tilde{z} \end{bmatrix}
\end{aligned}
\tag{15}
$$

where $\mathcal{R}_a := \mathcal{R} + k_p g_\star N_1 g_\star^\top + k_i \varepsilon g_\star g_\star^\top$, $b_a = -k_i \varepsilon \mathcal{R} g_\star - k_i N_1 g_\star - k_i N_2 g_\star - k_p k_i \varepsilon N_1 g_\star^\top Q g_\star g_\star^\top$. Invoking the condition (12), we have $\dot{W} < 0$. This implies that the closed-loop system is globally asymptotically stable. The proof is completed.

Note that the detailed analysis and description about the design of the PI controller around the passive output can be found in [24]. In this paper, we introduce a map defined in [25] to deal with the saturation problem of the control input for the boost converter. □

3.2. Reduced-Order Adaptive State Observer Design

For designing a reduced-order adaptive state observer, the system (1) can be expressed by

$$
\begin{aligned}
\dot{i} &= A_x i + b_x, & (16) \\
\dot{y} &= A_y i + \phi_y \eta_2, & (17)
\end{aligned}
$$

where $\eta_2 = G$ is an unknown constant, i is the non-measurable state, $y = v$ is the measurable output, and

$$
A_x = -\frac{r}{L}, b_x = \frac{-(1-u)y + E}{L}, A_y = \frac{1-u}{C}, \phi_y = -\frac{y}{C}.
$$

An adaptive state observer is proposed in the following proposition for estimating η_2 and i.

Assumption 1. *There exists a sequence of positive numbers $\{\delta_k\}_{k \in N}$ and a strictly increasing sequence of positive times $\{\tau_k\}_{k \in N}$ with $\tau \to \infty$ as $k \to \infty$ such that*

$$
\int_{\tau_k}^{\tau_{k+1}} m(s)m^\top(s)ds \geq \delta_k I_2.
\tag{18}
$$

where $\mathbb{I}_2$ denotes a 2×2 identity matrix.

Proposition 2. *The dynamic extension is designed as*

$$\dot{\xi}_y = A_x \xi_y + b_x,$$
$$\dot{X}_{A_x} = A_x X_{A_x}, X_{A_x}(0) = 1,$$

$$\dot{m} = -\lambda m + \lambda \begin{bmatrix} A_y X_{A_x} \\ \phi_y \end{bmatrix}, \tag{19}$$

$$\dot{\omega} = -\lambda\omega + \lambda(\lambda y + A_y \xi_y), \tag{20}$$

$$q = \lambda y - \omega = m^\top \eta. \tag{21}$$

The observer is designed as

$$\dot{\hat{\eta}} = -\gamma m(m^\top \hat{\eta} - q), \tag{22}$$

Partition the vector $\hat{\eta}$ *as* $\eta = \begin{bmatrix} \eta_1 & \eta_2 \end{bmatrix}^\top$. *The estimates* $\hat{i}$ *and* $\hat{G}$ *are given by*

$$\begin{cases} \hat{x}_1 = \xi_y + X_{A_x}\hat{\eta}_1, \\ \hat{G} = \hat{\eta}_2. \end{cases} \tag{23}$$

The following claim is satisfied, verifying the condition (18).

$$\lim_{t \to \infty} (\hat{i}(t), \hat{G}(t)) = (i(t), G(t)) \tag{24}$$

Proof. First, a new variable ξ_y is introduced to represent the dynamic extension of Equation (16), which is defined by

$$\dot{\xi}_y = A_x \xi_y + b_x. \tag{25}$$

Defining the error $e := i - \xi_y$ and combining (16) with (25), one has $\dot{e} = A_x e$. Based on the linear system theory, a state transition matrix X_{A_x} can be constructed by

$$\dot{X}_{A_x} = A_x X_{A_x}. \tag{26}$$

Then, we have $e = X_{A_x}\eta_1$, where $\eta_1 = e(0) = i(0) - \xi_y(0)$. In this case,

$$i = \xi_y + X_{A_x}\eta_1 \tag{27}$$

is obtained. Hence, to reconstruct i, the parameter η_1 related with the initial condition should be estimated. Now, it is noted that the state observation is transformed into the parameter estimation by using the dynamic extension technique. □

Next, to estimate the unknown constant η_1, η_2, the linear regressor equation (LRE) should be constructed. Toward the end, substituting Equation (27) in Equation (17) yields

$$\dot{y} = A_y(\xi_y + X_{A_x}\eta_1) + \phi_y \eta_2. \tag{28}$$

Then, a filter is applied in both sides of the above equation, which yields

$$\left[\frac{\lambda s}{s+\lambda}\right] y = \left[\frac{\lambda}{s+\lambda}\right] A_y \xi_y + \left[\frac{\lambda}{s+\lambda}\right] \left(\begin{bmatrix} A_y X_{A_x} & \phi_y \end{bmatrix} \begin{bmatrix} \eta_1 \\ \eta_2 \end{bmatrix}\right). \tag{29}$$

Then, we define

$$m := \left[\frac{\lambda}{s+\lambda} \right] \left(\begin{array}{c} A_y X_{A_x} \\ \phi_y \end{array} \right),$$

$$\omega := \left[\frac{\lambda}{s+\lambda} \right] y - \left[\frac{\lambda}{s+\lambda} \right] A_y \xi_y.$$

The above equations can be rewritten by the form of differential equations (DE), which are given by (19) and (20). The LRE can be expressed as

$$q = m^\top \eta, \tag{30}$$

where $q := \lambda y - \omega, \eta := \left[\begin{array}{cc} \eta_1 & \eta_2 \end{array} \right]^\top$. The observer is designed as (22). The observer error dynamics is given by

$$\dot{\tilde{\eta}} = -\gamma m m^\top \tilde{\eta}, \tag{31}$$

where $\tilde{\eta} := \hat{\eta} - \eta$. The solution of the latter equation is given by

$$\tilde{\eta} = e^{-\gamma \int_0^t m(s) m^\top (s) ds} \tilde{\eta}(0), \ \forall t \geq 0. \tag{32}$$

whose origin is asymptotically stable under Assumption 1. The proof is completed.

3.3. Adaptive Output Feedback Control Design

In this section, we combine the adaptive observer described in Proposition 2 with the saturated controller designed in (10) to form an output feedback control scheme.

Note that the controller (10) is only driven by the passive output $\tilde{y}$, which depends linearly on the state $\chi = \left[\begin{array}{cc} i & v \end{array} \right]^\top$ and non-linearly on the unknown conductance G. Hence, we write $\tilde{y}$ as

$$\tilde{y} = (C_0 + h_0(\eta_2))\chi + C_1 + h_1(\eta_2). \tag{33}$$

where the matrices $C_0 \in \mathbb{R}^{1 \times 2}, C_1 \in \mathbb{R}$ are independent of η_2 and $h_0(\eta_2) \in \mathbb{R}^{1 \times 2}, h_1(\eta) \in \mathbb{R}$ are—in general—nonlinear functions dependent on η_2. Note that $\tilde{y} = v_\star i - i_\star v$.

Substituting the estimated terms $\hat{i}$ and $\hat{\eta}_2$ in (35) yields

$$\hat{\tilde{y}} = (C_0 + h_0(\hat{\eta}_2))\hat{\chi} + C_1 + h_1(\hat{\eta}_2), \tag{34}$$

where $\hat{\chi} = \left[\begin{array}{cc} \hat{i} & v \end{array} \right]^\top$. It can be also expressed in the disturbed form

$$\hat{\tilde{y}} = \tilde{y} + \delta(\hat{\eta}_2, \hat{\chi}), \tag{35}$$

where

$$\delta(\hat{\eta}_2, \hat{\chi}) := (C_0 + h_0(\eta_2))(\hat{\chi} - \chi) + (h_0(\hat{\eta}_2) - h_0(\eta_2))\hat{\chi} + h_1(\hat{\eta}_2) - h_1(\eta_2)$$

is viewed as a disturbance signal. We notice that $\delta(\eta_2, \chi) = 0$; hence, the proposed adaptive observer ensures

$$\lim_{t \to \infty} \delta(\hat{\eta}_2(t), \hat{\chi}(t)) = 0.$$

The following proposition will establish the stability analysis of the closed-loop system under the output feedback controller.

Proposition 3. *Consider the system* (5) *with the measurable output y. The closed-loop system under the output feedback controller,*

$$\dot{z} = \hat{\tilde{y}}, \tag{36a}$$

$$u = q(-k_p\hat{\tilde{y}} - k_i z) \tag{36b}$$

with $\hat{\tilde{y}}$ defined in (34), *is (locally) asymptotically stable for all $k_p > 0, k_i > 0$.*

Proof. First, invoking (35), the output feedback controller (36) can be written as

$$\dot{z} = \tilde{y} + \delta, \tag{37a}$$

$$u = q(-k_p\tilde{y} - k_i z - k_p\delta). \tag{37b}$$

Invoking the assumption (8), one has

$$u = q(w - k_p\delta) = q(w) + \psi(w, k_p\delta) \tag{38}$$

where $w = -k_p\tilde{y} - k_i z$. Substituting (37) and (38) in system (5) yields the closed-loop system

$$\begin{bmatrix} \dot{\tilde{x}} \\ \dot{\tilde{z}} \end{bmatrix} = \begin{bmatrix} Ju - R - k_p N_1 g_\star g_\star^\top & -N_1 g_\star \\ g_\star^\top & 0 \end{bmatrix} \nabla \bar{W} - \Psi, \tag{39}$$

where

$$\Psi = \begin{bmatrix} g_\star \psi \\ \delta \end{bmatrix}.$$

Note that Ψ is a disturbance signal.

$$\bar{W}(\tilde{x}, \tilde{z}) := \frac{1}{2}\tilde{x}^\top Q\tilde{x} + \frac{1}{2}\tilde{z}^\top k_i N_1 \tilde{z}.$$

The system (39) with $\Psi = 0$ is asymptotically stable. Note that $\lim_{t \to \infty} \Psi = 0$. With the help of the common result of the locally asymptotically stability of cascade system given in [30], the locally asymptotically stability of the system (39) is established. □

4. Simulation Results

In this section, the simulation results of the boost converter will be provided to assess the performance of the presented controller. The circuit parameters of the system are coincident with these of the experimental study, which are shown in Table 1. The control structure is revealed in Figure 2.

The set $\mathcal{U} \subset [0\ 1]$. To guarantee that the control input is maintained within such bounds, we complement the design by introducing a map $q : \mathbb{R} \to [u_n\ u_m]$ given by

$$q(s) = \frac{u_M - u_m}{2} \cdot \tanh(\tau s - u_0) + \frac{u_M + u_m}{2}, u_0 = \tau u_\star + \tanh^{-1}\left(\frac{u_M + u_m - 2u_\star}{u_M - u_m}\right) \tag{40}$$

In this simulation, we select $u_m = 0.1, u_M = 0.9$. The gains are chosen as $k_p = 0.05$, $k_i = 0.001, \gamma = 1, \mu = 0.1$ and initial conditions are given as $x_1(0) = L$ A, $x_2(0) = 2C$ V, $\xi_y(0) = 0, \hat{\eta}(0) = \begin{bmatrix} 0 & 0 \end{bmatrix}^\top, m(0) = \begin{bmatrix} 0 & 0 \end{bmatrix}^\top, w(0) = 0.$

Table 1. Simulation/experimental set-points and physical parameters.

Parameter	Symbol (Unit)	Value
Input voltage	E (V)	6
Reference output voltage	$x_{2\star}$ (V)	12
Gain	$x_{2\star}/E$	2
Parasitic resistance	r (Ω)	0.2
Conductance	G (s)	0.1
Inductance	L (μH)	28
Capacitance	C (μF)	830
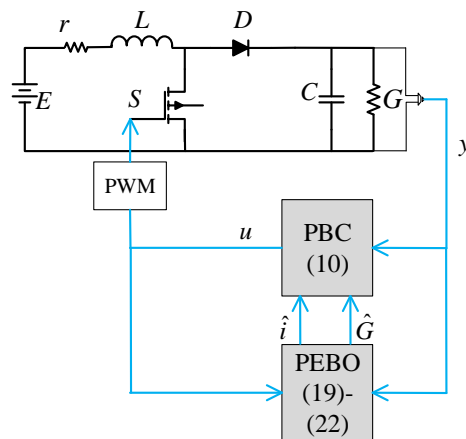
**Figure 2.** The control structure of boost converter under the proposed controller.

First, we want to test the transient of the closed-loop system under the different gain. It is observed from Figure 3 that a larger gain k_p, k_i will obtain a better transient. However, the trade-off between the transient and noise level should be considered during the selection of the gains. One sees that the traces of the output voltage v indeed coincide with the reference after the transient. In fact, we can see that the fluctuation of the current is a little large. Our next work will focus on this topic to deal with the current constraint problem. Note that the saturation of the control input u is ensured. Indeed, u belongs to the set [0.1 0.9]. As predicted by theory, the estimates $\hat{i}$, $\hat{G}$ converge to their real values, which makes the output voltage stay around the desired value.

Next, we want to check the difference between the controller with the saturation and without it. Toward this, we remove the saturation and do not change any other equations. In the case, the response curves of the two cases are presented in Figure 4. It is seen that the trace of the control input u without the saturation is obviously beyond the constraint [0 1]. This is detrimental to the practical applications. Indeed, a forced saturation function added in control input will reduce the performance and does not ensure the stability in the experimental test. In our design, the strictly stability analysis with the saturation is given. As shown in the figure, we can see the control input nicely satisfies the constraint [0.1 0.9].

Finally, we want to check the robustness performance against the variation of the conductance G. To this end, a step change is added in G, which ranges from 0.1 [s] to 0.2 [s]. The traces of the state and the estimate $\hat{G}$ can be observed in Figure 5. Along with the increasing of the gain λ, the estimate $\hat{G}$ will have a quick convergence. This results in the output voltage also capturing a better transient.
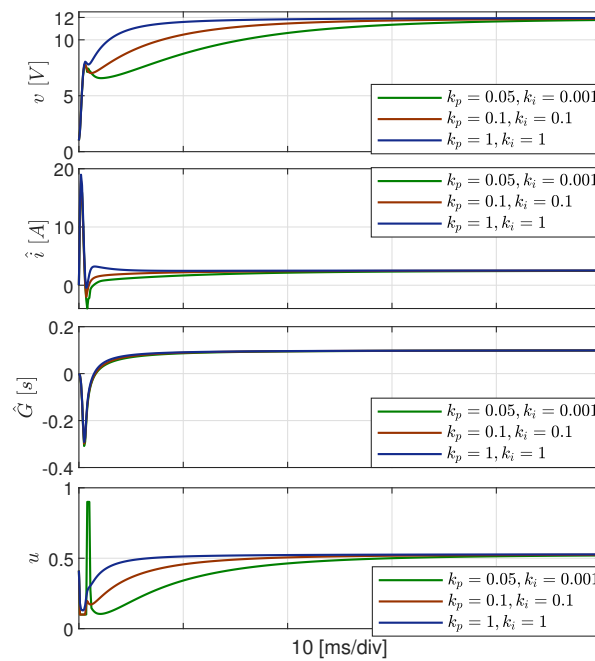
Figure 3. The response curves of boost converter under the proposed controller with different gain.
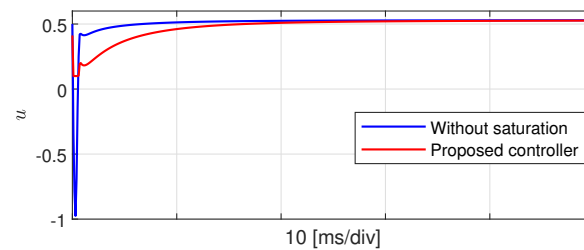
Figure 4. The zooms of the controller inputs with the saturation and without it.
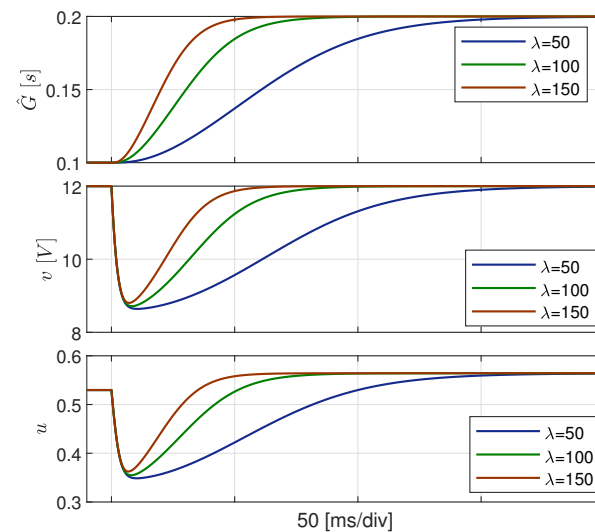
Figure 5. The response curves of the proposed controller in the presence of the change in *G*.

Figure 6. The experimental setup of boost converter.

5. Experiment Results

In this section, the experimental results of a boost converter are shown to validate the theoretical claims. The boost converter is developed using the TI MSP430F5132 MCU using the code composer studio (CCS) to implement the controller. The switching frequency is 120 KHz. The IRFP4568 N-Channel MOSFET and the STPS6045C Schottky diode are used for the converter circuit design. The picture of the experimental setup is shown in Figure 6. The selections of the control gain and initial conditions are similar to those of the simulation study.

The operation curves of the boost converter are shown in Figure 7. It is seen that the output voltage stays around the desired value. The estimates $\hat{i}$ and $\hat{G}$ are consistent with the real values. The transient of the boost converter is shown in Figure 8. Note that it takes 50 ms to converge to the equilibrium. The curves of the PI controller are revealed in Figure 9. It is observed that the transient of the PI control is poor, and the convergence time is 0.25 s. Therefore, it is concluded that the transient of the proposed controller has an advantage over that of the PI controller.

Next, the step change in the reference is considered, which changes from 10 V to 16 V. The estimate $\hat{G}$ is around 0.2 s. The result is shown in Figure 10. One sees that the output voltage nicely converges to the changing reference. A step change in G is added so that the robustness performance can be tested in Figure 11. We can see that the output voltage can stay at 12 V in the presence of the variation of G. Hence, the nice transient and robustness performance of the proposed controller are tested.
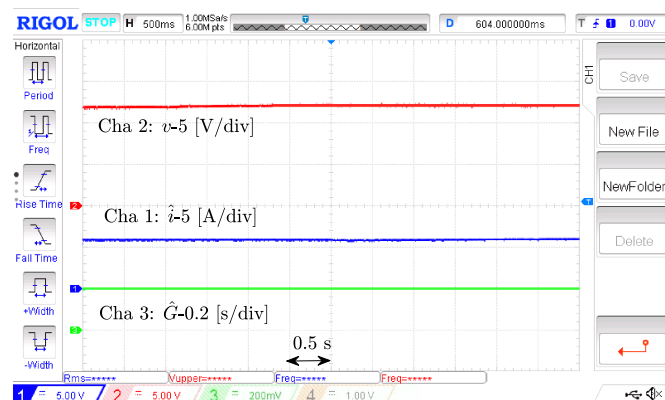

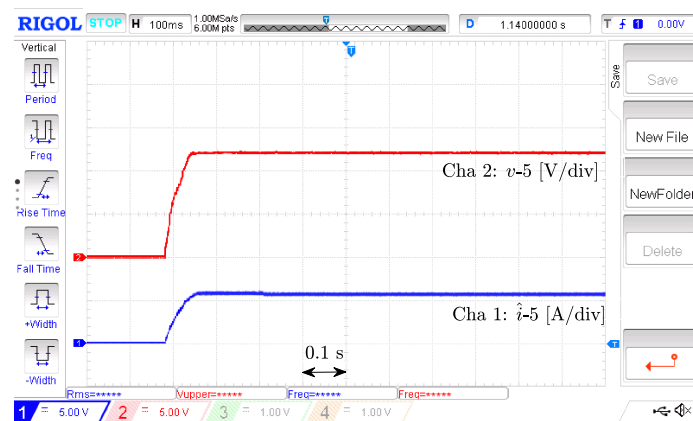**Figure 7.** The operation curves of boost converter under the proposed controller.

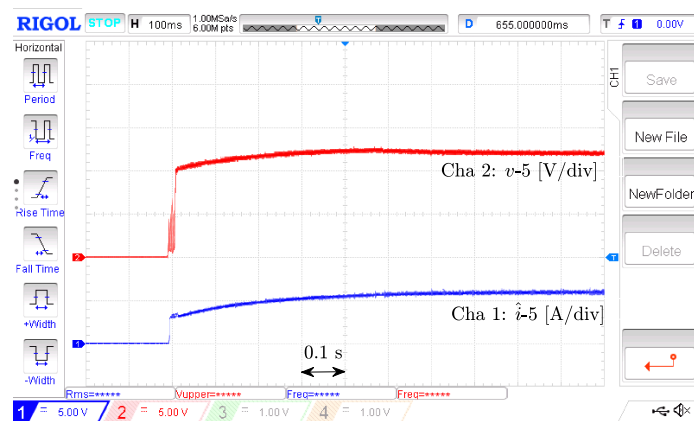**Figure 8.** The transient of boost converter under the proposed controller.

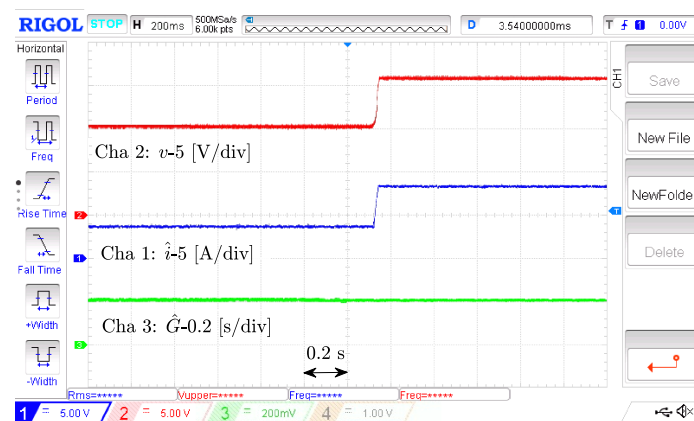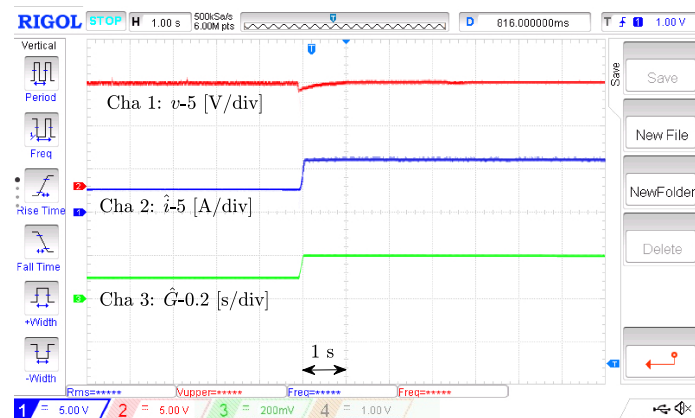**Figure 9.** The transient of boost converter under the PI controller.

Figure 10. The response curves of boost converter under the proposed controller in the presence of a step change in the reference.

Figure 11. The response curves of boost converter under the proposed controller in the presence of a step change in *G*.

6. Conclusions and Future Work

The output feedback control problem of boost converter with unknown load conductance was solved. Invoking the passivity property of the system, a saturated controller was proposed with the strict stability analysis. Moreover, a reduced-order observer was designed to estimate the current and load conductance. In this case, an output feedback controller was proposed. The simulation and experimental results under the designed controller were given. The future work will focus on the current constraint problem.

Author Contributions: Conceptualization, W.H.; methodology, W.H.; software, Y.Z.; validation, X.Z.; formal analysis, W.H.; investigation, X.Z.; data, X.Z.; writing—original draft preparation, X.Z.; writing—review and editing, W.H.; supervision, W.H.; project administration, W.H.; funding acquisition, W.H. All authors have read and agreed to the published version of the manuscript.

Institutional Review Board Statement: Not applicable.

Informed Consent Statement: Not applicable.

Data Availability Statement: Not applicable.

Conflicts of Interest: The authors declare no conflict of interest.

References

1. Hossain, M.; Rahim, N. Recent progress and development on power DC-DC converter topology, control, design and applications: A review. *Renew. Sustain. Energy Rev.* **2018**, *81*, 205–230. [CrossRef]
2. Raghavendra, K.V.G.; Zeb, K.; Muthusamy, A.; Krishna, T.; Kumar, S.; Kim, D.H.; Kim, M.S.; Cho, H.G.; Kim, H.J. A comprehensive review of DC–DC converter topologies and modulation strategies with recent advances in solar photovoltaic systems. *Electronics* **2020**, *9*, 31. [CrossRef]
3. He, W.; Namazi, M.M.; Li, T.; Ortega, R. A state observer for sensorless control of power converters with unknown load conductance. *IEEE Trans. Power Electron.* **2022**. [CrossRef]
4. Ahmad, S.; Ali, A. Active disturbance rejection control of DC–DC boost converter: A review with modifications for improved performance. *IET Power Electron.* **2019**, *12*, 2095–2107. [CrossRef]
5. Reddy, D.S. Review on power electronic boost converters. *Aust. J. Electr. Electron. Eng.* **2021**, *18*, 127–137. [CrossRef]
6. Santi, E.; Monti, A.; Li, D.; Proddutur, K.; Dougal, R.A. Synergetic control for DC-DC boost converter: Implementation options. *IEEE Trans. Ind. Appl.* **2003**, *39*, 1803–1813. [CrossRef]
7. Leon-Masich, A.; Valderrama-Blavi, H.; Bosque-Moncusí, J.M.; Maixe-Altes, J.; Martínez-Salamero, L. Sliding-mode-control-based boost converter for high-voltage–low-power applications. *IEEE Trans. Ind. Electron.* **2014**, *62*, 229–237. [CrossRef]

8. Oucheriah, S.; Guo, L. PWM-based adaptive sliding-mode control for boost DC–DC converters. *IEEE Trans. Ind. Electron.* **2012**, *60*, 3291–3294. [CrossRef]
9. Tong, Q.; Zhang, Q.; Min, R.; Zou, X.; Liu, Z.; Chen, Z. Sensorless predictive peak current control for boost converter using comprehensive compensation strategy. *IEEE Trans. Ind. Electron.* **2013**, *61*, 2754–2766. [CrossRef]
10. Wang, J.; Li, S.; Fan, J.; Li, Q. Nonlinear disturbance observer based sliding mode control for PWM-based DC-DC boost converter systems. In Proceedings of the 27th Chinese Control and Decision Conference (2015 CCDC), Qingdao, China, 23–25 May 2015; pp. 2479–2484.
11. Sira-Ramirez, H.J.; Silva-Ortigoza, R. *Control Design Techniques in Power Electronics Devices*; Springer Science & Business: London, UK, 2006.
12. Chincholkar, S.; Jiang, W.; Chan, C.Y.; Rangarajan, S. A Simplified Output Feedback Controller for the DC-DC Boost Power Converter. *Electronics* **2021**, *10*, 493. [CrossRef]
13. Sira-Ramírez, H.; Oliver-Salazar, M.A.; Leyva-Ramos, J. Voltage regulation of a fuel cell-boost converter system: A proportional integral exact tracking error dynamics passive output feedback control approach. In Proceedings of the 2012 American Control Conference (ACC), Montreal, QC, Canada, 27–29 June 2012; pp. 2153–2158.
14. Chan, C.Y. Simplified parallel-damped passivity-based controllers for dc–dc power converters. *Automatica* **2008**, *44*, 2977–2980. [CrossRef]
15. Son, Y.I.; Kim, I.H. Complementary PID controller to passivity-based nonlinear control of boost converters with inductor resistance. *IEEE Trans. Control. Syst. Technol.* **2011**, *20*, 826–834. [CrossRef]
16. Rodriguez, H.; Ortega, R.; Escobar, G.; Barabanov, N. A robustly stable output feedback saturated controller for the boost DC-to-DC converter. *Syst. Control. Lett.* **2000**, *40*, 1–8. [CrossRef]
17. Wang, C.; Li, R.; Su, X.; Shi, P. Output Feedback Sliding Mode Control of Markovian Jump Systems and Its Application to Switched Boost Converter. *IEEE Trans. Circuits Syst. Regul. Pap.* **2021**, *68*, 5134–5144. [CrossRef]
18. Ma, G.; Qin, L.; Liu, X.; Wu, G. Event-triggered output-feedback control for switched linear systems with applications to a boost converter. In Proceedings of the 2016 IEEE 11th Conference on Industrial Electronics and Applications (ICIEA), Hefei, China, 5–7 June 2016; pp. 2431–2436.
19. Kim, S.K.; Kim, J.S.; Park, C.R.; Lee, Y.I. Output-feedback model predictive controller for voltage regulation of a DC/DC converter. *IET Control. Theory Appl.* **2013**, *7*, 1959–1968. [CrossRef]
20. Salhi, B.; El Fadil, H.; Ahmed Ali, T.; Magarotto, E.; Giri, F. Adaptive output feedback control of interleaved parallel boost converters associated with fuel cell. *Electr. Power Components Syst.* **2015**, *43*, 1141–1158. [CrossRef]
21. Jaafar, A.; Alawieh, A.; Ortega, R.; Godoy, E.; Lefranc, P. PI stabilization of power converters with partial state measurements. *IEEE Trans. Control. Syst. Technol.* **2012**, *21*, 560–568. [CrossRef]
22. Tavan, M.; Sabahi, K.; Hajizadeh, A.; Soltani, M.N.; Jessen, K. Overcoming the Detectability Obstacle in Adaptive Output Feedback Control of DC-DC Boost Converter With Unknown Load. *IEEE Trans. Control. Syst. Technol.* **2020**, *29*, 2678–2686. [CrossRef]
23. Zhang, X.; Martinez-Lopez, M.; He, W.; Shang, Y.; Jiang, C.; Moreno-Valenzuela, J. Sensorless Control for DC–DC Boost Converter via Generalized Parameter Estimation-Based Observer. *Appl. Sci.* **2021**, *11*, 7761. [CrossRef]
24. Ortega, R.; Romero, J.G.; Borja, P.; Donaire, A. *PID Passivity-Based Control of Nonlinear Systems with Applications*; John Wiley & Sons: Hoboken, NJ, USA, 2021.
25. Zonetti, D.; Bergna-Diaz, G.; Ortega, R.; Monshizadeh, N. PID passivity-based control of power converters: Large-signal stability, robustness and performance. *arXiv* **2021**, arXiv:2101.05047.
26. Ortega, R.; Bobtsov, A.; Pyrkin, A.; Aranovskiy, S. A parameter estimation approach to state observation of nonlinear systems. *Syst. Control. Lett.* **2015**, *85*, 84–94. [CrossRef]
27. Middlebrook, R.D.; Cuk, S. A general unified approach to modelling switching-converter power stages. In Proceedings of the 1976 IEEE Power Electronics Specialists Conference, Cleveland, OH, USA, 8–10 June 1976; pp. 18–34.
28. Middlebrook, R.D.; Ćuk, S. A general unified approach to modelling switching-converter power stages. *Int. J. Electron. Theor. Exp.* **1977**, *42*, 521–550. [CrossRef]
29. Erickson, R.W.; Maksimovic, D. *Fundamentals of Power Electronics*; Springer Science & Business: Cham, Germany, 2007.
30. Sepulchre, R.; Jankovic, M.; Kokotovic, P.V. *Constructive Nonlinear Control*; Springer Science & Business: London, UK, 2012.